J Biomed Eng Syst Technol Low Middle Income Ctries 2026; 1(1): 45–56

Journal of Biomedical Engineering Systems and Technologies for Low- and Middle-Income Countries

Early Cardiovascular Disease Detection: An Improved Pan-Tompkins Algorithm for QRS Detection in Electrocardiogram

Ahadzi E[1*], Hasmin SD[1] , Acquah I[1] , Adjei PE[1]

[1] Department of Computer Engineering, College of Engineering, Kwame Nkrumah University of Science and Technology, Kumasi, Ghana

[*] Corresponding author: Eyram Ahadzi (email: eyramahadzi8@gmail.com)

Abstract

Cardiovascular diseases (CVDs) are the leading cause of death globally, with low- and middle-income countries (LMICs) bearing the greatest burden. Electrocardiograms (ECGs), which reflect the heart's electrical activity, are an essential tool in diagnosing CVD. The QRS complex is the most prominent wave in an ECG signal and is used for evaluating the overall heart function of an individual. The Pan-Tompkins algorithm is widely used for the detection of QRS complexes. It is, however, susceptible to baseline wander noise, has decreased sensitivity for diverse ECG morphologies, and exhibits real-time delay, leading to its suboptimal performance in QRS complex detection. This study presents an improved Pan-Tompkins approach that combines the strengths of the Pan-Tompkins algorithm with a Recurrent Neural Network (RNN) to deliver more accurate and efficient QRS detection. The proposed algorithm achieved precision, recall, and F1-scores above 96% on Lead II of the MIT-BIH Arrhythmia Database. Overall, false positive and false negative rates were below 0.05%, calculated across the selected segments from all patient records. Execution time was reduced by 4% relative to the original Pan–Tompkins algorithm on identical ECG segments, directly lowering latency and improving real-time performance. A band-pass filter of 6–16 Hz was used, which improved robustness against baseline wander, effectively reducing noise. The algorithm demonstrated enhanced resilience to morphological variability in ECG signals, ensuring more reliable detection across diverse patterns. By integrating this AI-driven algorithm into low-cost, portable ECG devices, there is strong potential to support early detection of CVDs, particularly in underserved areas. This work contributes to a practical, scalable solution that can help strengthen digital health infrastructure and improve clinical outcomes in LMICs.

Keywords; *Cardiovascular Diseases, QRS complex, R peak detection, Electrocardiogram, Pan-Tompkins Algorithm, Recurrent Neural Networks.*

editor@best-lmic.org, www.best-lmic.org Post Office BOX 00800-13975, Westlands, Nairobi, Kenya.

1. Introduction

According to the World Health Organization (WHO), cardiovascular diseases (CVDs) stand as the leading cause of global mortality, resulting in nearly 25.6 million deaths in 2020.[1] More than 80% of CVD deaths occur in low- and middle-income countries (LMICs), highlighting the severity of the burden in these regions.[2] While high-income countries (HICs) have seen a decline in CVD-related deaths, LMICs are experiencing a continuous rise, with annual mortality rates reaching approximately 300 to 600 deaths per 100,000 people.[3] One significant and often undiagnosed subgroup of CVDs is cardiac arrhythmias, which involve irregularities in the heart's rhythm.[4,5] These conditions, including atrial fibrillation, can lead to serious complications such as stroke and heart failure, or sudden cardiac death if not detected early.[5]

Electrocardiograms (ECGs) play a vital role in the detection of CVDs, as they reflect the electrical activity of the heart and consist of a P wave, a QRS complex, and a T segment,[6] which shows normal rhythm. The P wave is representative of the contraction of the atria, the QRS complex corresponds to ventricular contraction, and the T wave is representative of the repolarization of the ventricles.

Among the ECG waveforms, the QRS (Figure 1) complex is the most pronounced wave, providing information on heart rate and rhythm abnormalities.[7]

Accurate and timely detection of the QRS complex is therefore essential for diagnosing rhythm conditions, including various forms of arrhythmias, as well as other cardiac conditions such as myocardial infarction.[7] Before the emergence of wearable technologies, the Pan-Tompkins algorithm stood out as a simple yet widely used method for QRS detection.[7,8]

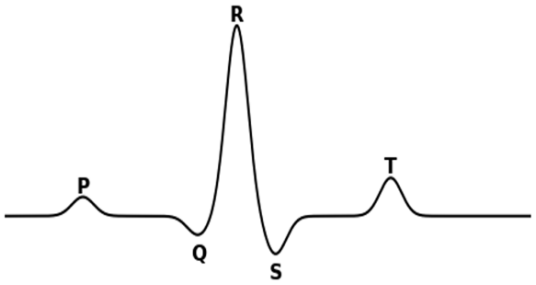

Figure 1. *ECG signal depicting PQRST morphology.*

Although generally accurate, the algorithm faces challenges in the presence of noise, diverse morphologies of the ECG,[9] or unusual, and wider QRS complexes.[10] Moreover, it introduces real-time processing delays and demonstrates suboptimal accuracy when accessing publicly accessible data.[8] As wearable devices evolve, the volume of ECGs generated for analysis increases, emphasizing the need for more efficient algorithms.[11] These drawbacks significantly hinder its performance in mobile and wearable devices, which are increasingly important in LMICs where healthcare access is limited and early diagnosis is crucial.

To address the aforementioned limitations, this study proposes an improved Pan-Tompkins algorithm that combines the Pan-Tompkins with Machine Learning (ML), specifically Recurrent Neural Networks (RNNs). The goal is to improve morphological robustness, mitigate the effects of baseline wander noise, and reduce latency, thereby enabling faster and more accurate QRS detection. By integrating this AI-enhanced algorithm into portable, mobile-platform-based ECG devices, the solution offers a practical pathway toward scalable and reliable CVD diagnostics, particularly in underserved regions.

2. Related Works

This section reviews research efforts focused on enhancing the Pan-Tompkins algorithm (Figure 2) for improved QRS detection. The Pan-Tompkins algorithm remains a foundational approach in QRS detection. It leverages a multi-stage processing pipeline to identify the characteristic R peak within the QRS complex. It consists of two phases: a pre-processing phase, which involves **filtering, differentiation, squaring**, and **integration**, and a decision-making phase, by applying two thresholds for **R peak detection**.[12]

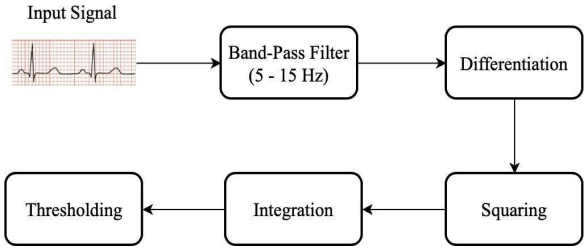

Figure 2. *Block Diagram for Pan-Tompkins Algorithm.*

In the first stage, the ECG signal undergoes filtering using a cascaded high-pass and low-pass filter combination. This filtering process, as described by Pan and Tompkins, serves as a noise rejection mechanism, attenuating unwanted frequencies outside the bandwidth of interest for QRS complexes. The low-pass filter gets rid of signals of higher frequencies, whereas the high-pass filter gets rid of signals of lower frequencies.

Low-pass filter equation:

$$y(nT) = 2y(nT - T) - y(nT - 2T) + x(nT) - 2x(nT - 6T) + x(nT - 12T) \quad (1)$$

High-pass filter equation:

$$y(nT) = 32x(nT - 16T) - [y(nT - T) + x(nT) - x(nT - 32T)] \quad (2)$$

Bandpass filter equation:

$$y_{bandpass}(nT) = Highpass(LowPass(x(nT))) \quad (3)$$

where $y(nT)$: filtered signal, $x(nT)$: input signal, and T: sampling period.

The signal is then differentiated from point to point to highlight the rapid changes associated with QRS complexes. The positive and negative deflections of the differentiated signal are then squared. This makes the data point positive and non-linearly amplifies the derivative output.

The signal is then passed through a moving window integrator to obtain the waveform feature in addition to the slope of the R-wave. This integration stage extracts the overall waveform features while preserving the slope information. For R peak detection, Pan and Tompkins used a dual threshold to discriminate the location of the QRS complexes. These thresholds dynamically adjust based on the characteristics of the filtered signal. The higher of the two thresholds (Threshold 1) is used in the first assessment of the signal. If no R-peak is detected within a pre-determined period, the lower threshold (Threshold 2) is applied, necessitating the use of a search-back approach to look back in time for the QRS complex.[12,13]

Despite its effectiveness, the algorithm struggles with baseline wander, irregular morphologies[10] and performance in wearable technologies.[8]

To address these challenges, the Hamilton-Tompkins algorithm refined peak detection rules by incorporating median filtering and peak level estimation. While this approach reduced false positives, it still exhibited limitations in noise-prone environments.[8]

Similarly, wavelet transform-based methods combine Pan-Tompkins with multiscale analysis to improve the detection of atypical QRS morphologies. These approaches enhance adaptability but often suffer from increased computational complexity and susceptibility to noise amplification.[7]

Imtiaz and Khan, using Pan Tompkins++, introduced modifications such as an

expanded 5–18 Hz bandpass filter and an additional threshold to improve detection sensitivity. However, its reliance on more thresholds and filters risks latency.[9]

The AccYouRate Modified Pan-Tompkins Algorithm (AMPT) simplifies detection by using only the final filtered signal, improving clarity but reducing adaptability to signals with high amplitude variation.[10]

Overall, while each variation aims to enhance detection, challenges with noise resilience, morphological adaptability, and real-time performance persist. These limitations motivate the improved Pan-Tompkins approach proposed in this study, which integrates Recurrent Neural Networks (RNNs) with the Pan-Tompkins algorithm to enhance the robustness and efficiency of QRS detection.

3. Materials and Methods

a. Dataset

The MIT-BIH Arrhythmia Database, a widely recognized and valuable resource for cardiac signal analysis, was utilized for this study and comprises 48 half-hour snippets of 2-channel (Lead II and Lead V5) ECG recordings made from 47 people sampled at 360 Hz,[3,9] resulting in approximately 60,000 samples per record. Each record includes beat annotations and rhythm information, with a range of arrhythmic conditions such as premature ventricular contractions (PVCs), atrial fibrillation, and normal sinus rhythm. The dataset includes detailed annotations on a beat-by-beat basis, enabling precise evaluation of detection algorithms. It also contains segments of normal sinus rhythm with clearly defined P waves, QRS complexes, and T waves. This combination of normal and abnormal rhythms supports the development and evaluation of models across a broad spectrum of cardiac conditions.[1] While not all patient records contain arrhythmias, the dataset as a whole spans a wide range of rhythm types, ensuring that algorithm performance was evaluated across both normal and arrhythmic conditions.

b. Data Preprocessing

The preprocessing approach adopted in this study is based on the Pan-Tompkins algorithm, with a key modification aimed at improving QRS detection performance. A band-pass filter with a frequency range of 6 – 16 Hz was applied, replacing the 5 – 15 Hz range.

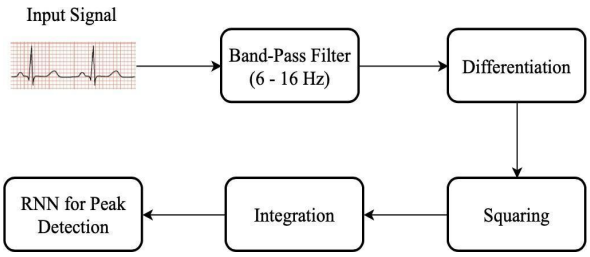

Figure 3. *Block Diagram for Improved Pan-Tompkins Algorithm.*

Following filtering, the signal was differentiated, squared, and passed through a moving window integrator. These stages are consistent with the Pan-Tompkins algorithm.

c. Peak Detection

This study uses a recurrent neural network (RNN) model to enhance R-peak detection. RNNs have shown a superior ability to model sequential data such as ECG signals due to their inherent temporal dependencies and the ability to retain contextual information in time steps,[14] which are critical for accurate identification of complex QRS. They also tend to require less computational resources than transformer-based models, making them practical for deployment in low-resource and real-time settings.

All experiments were conducted on a

MacBook Pro with a 1.4 GHz Quad-Core Intel Core i5 processor and on Google Colab with a T4 GPU, using Python 3.12 and TensorFlow 2.16. The architecture consisted of an initial Conv1D layer (64 filters, kernel size 3, ReLU activation), followed by Batch Normalization, MaxPooling1D and Dropout for feature extraction and regularization. Two stacked bidirectional Long Short-Term Memory (LSTM) layers (128 units each) captured temporal dynamics, followed by dense layers with dropout and L2 regularization, and a final sigmoid output layer for classification of R-peaks (Figure 4). The classification task was framed as a binary decision problem, where each 128-sample window was labeled 1 if it contained an annotated R-peak (based on the ground truth annotations from the MIT-BIH Arrhythmia Database) and 0 otherwise.

The RNN model was trained using Lead II ECG data with the first 50,000 samples from each subject to ensure a representative dataset for capturing diverse cardiac events while optimizing computational efficiency. The dataset was split into training (70%), validation (20%), and test (10%) subsets in a segment-based manner, which may slightly overestimate generalization performance. Given the diverse range of rhythms in the MIT-BIH database, including both arrhythmic and non-arrhythmic patterns, this test set composition was essential for evaluating the model's R-peak detection performance across various cardiac conditions, thereby supporting its potential applicability in broader diagnostic settings.

The training process involved 10 epochs with a linearly decaying learning rate starting from 0.001, achieving an accuracy of 97.70% on the test set.

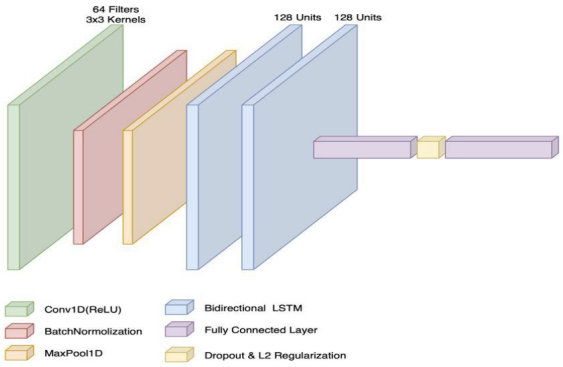

Figure 4. *RNN-based architecture for R-peak detection.*

d. Model Application

The ECG signals from the MIT-BIH Arrhythmia Database, sampled at 360 Hz, underwent standard preprocessing steps including filtering, differentiation, squaring, and moving window integration as per the Pan-Tompkins algorithm. However, to enable the trained RNN model to work on datasets with varying sampling rates, signals were resampled to 360 Hz during peak detection. This resampling ensures compatibility with the model's input requirements and may facilitate adaptation to ECG signals from sources with varying sampling rates.

To facilitate practical application, the trained model was saved and can be used for predictions without the need for retraining. For future predictions, the saved model can be applied directly to resampled and filtered ECG signals using the same pre-processing steps. This approach streamlines the process and ensures consistent results across datasets, regardless of their original sampling rate. Furthermore, to improve the accuracy of peak detection, a search-back mechanism was implemented to address potential missing peaks. This method involves scanning backward from each detected peak to ensure that no peaks are overlooked, thus enhancing the reliability of the peak detection process.

e. Experimental Configurations

We evaluated the effectiveness of our proposed method in detecting R peaks using three experimental configurations. The first setup involved the Pan-Tompkins algorithm, implemented as a baseline for R-peak detection. The second configuration used the Recurrent Neural Network (RNN) applied directly without traditional preprocessing steps such as bandpass filtering or differentiation. This setup served to evaluate the model's ability to detect R-peaks without any preprocessing and provided insight into how much preprocessing contributes to performance. The third configuration, referred to as the improved Pan-Tompkins algorithm method, combined Pan-Tompkins-inspired preprocessing (bandpass filtering between 6–16 Hz, differentiation, squaring, and moving window integration) with the RNN for R peak detection.

To support qualitative and quantitative evaluation, multiple ECG signal segments were randomly selected from different patient records. One signal segment was used to visually demonstrate the transformation process through each stage of the algorithm, from the original ECG signal to final R-peak detection. Additionally, four signal segments from four different patients were used to compare R-peak detection performance across the three experimental configurations.

To assess baseline wander removal, ten ECG signal segments from ten different patients were randomly selected. For each segment, the standard deviation (SD) of the baseline component was computed for the raw signal, the Pan-Tompkins filtered signal, and the signal processed using our improved bandpass filtering approach. The SD values obtained from the Pan-Tompkins and improved methods were then compared using a paired t-test, with the corresponding p-value calculated to determine the statistical significance of the observed difference in baseline suppression. For qualitative illustration, two representative segments from these ten were selected to visually compare the unfiltered signal, the Pan-Tompkins filtered output, and the improved Pan-Tompkins filtered result. Quantitative performance metrics were computed using the entire ECG recordings from all patient records across both leads to ensure robustness and generalizability. However, to assess average execution time, a consistent representative segment was extracted from each record and used uniformly across all configurations.

4. Results

The effectiveness of our improved algorithm was assessed using standard performance metrics, including sensitivity, precision, F1 score, false negative rate (FNR), false positive rate (FPR), and average execution time. These metrics were evaluated on all ECG recordings across both leads from the MIT-BIH Database, as summarized in Table 1 for Lead II and Table 2 for Lead V5. Standard deviation noise (SDN) and baseline wander are not independent, with baseline wander partly contributing to SDN.[15] A decrease in standard deviation reflects a reduction in baseline wander, indicating lower variability in the ECG signal. Accordingly, standard deviation was used to assess baseline drift, with lower values suggesting reduced wander and improved signal quality, as presented in Table 3. Figure 5 shows the signal at different stages of our improved algorithm.

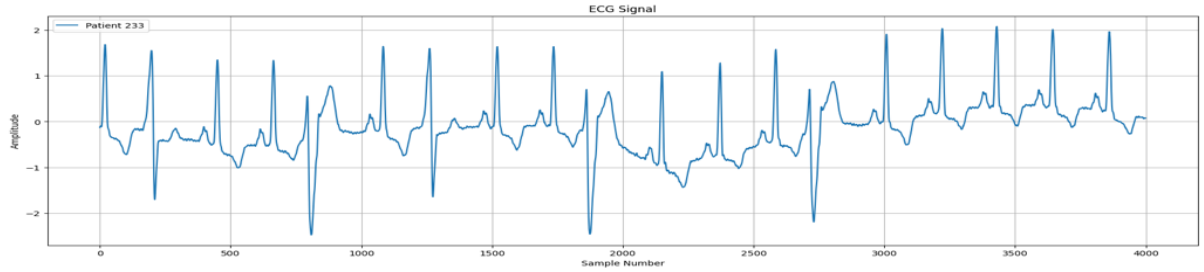

(a)

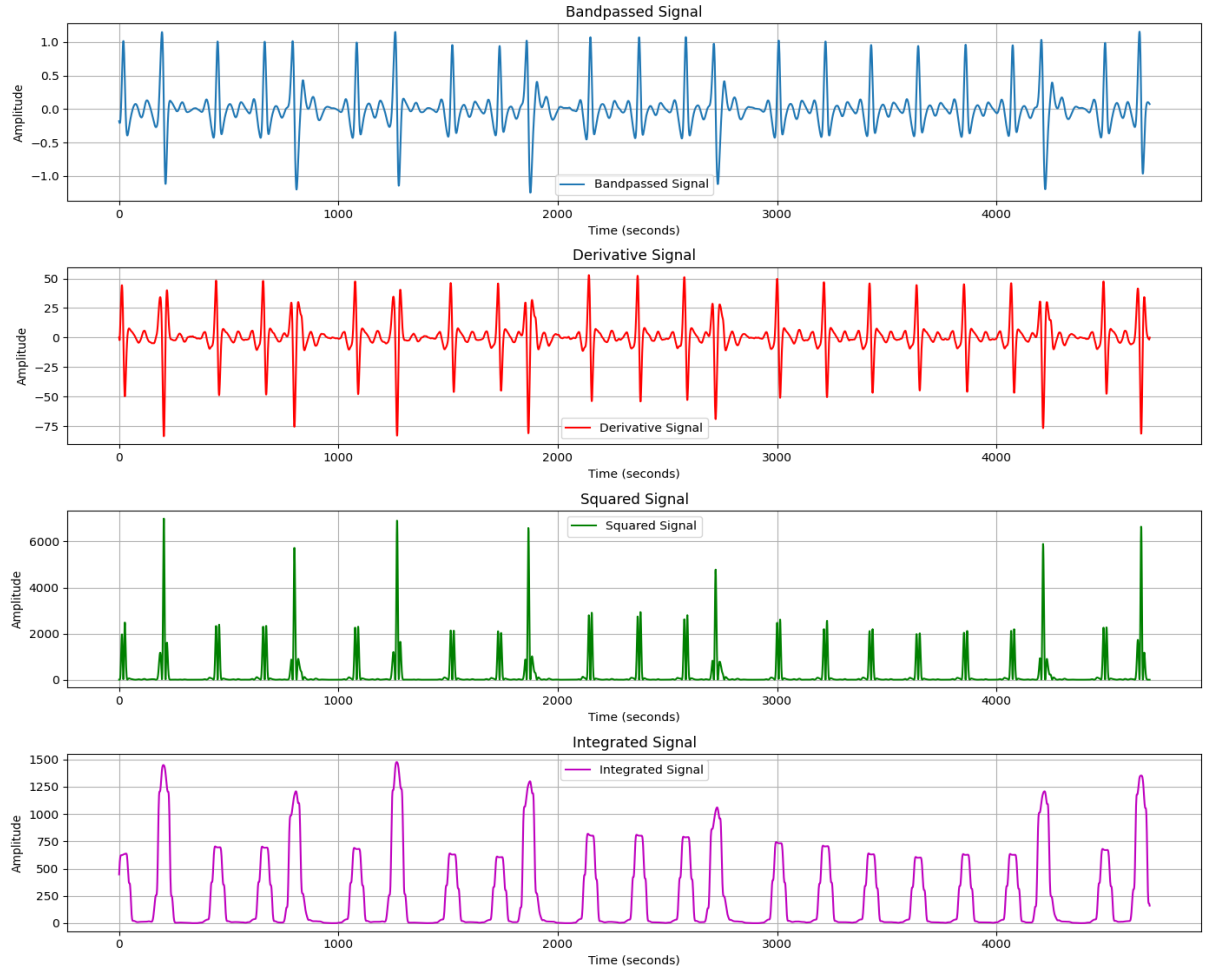

(b)

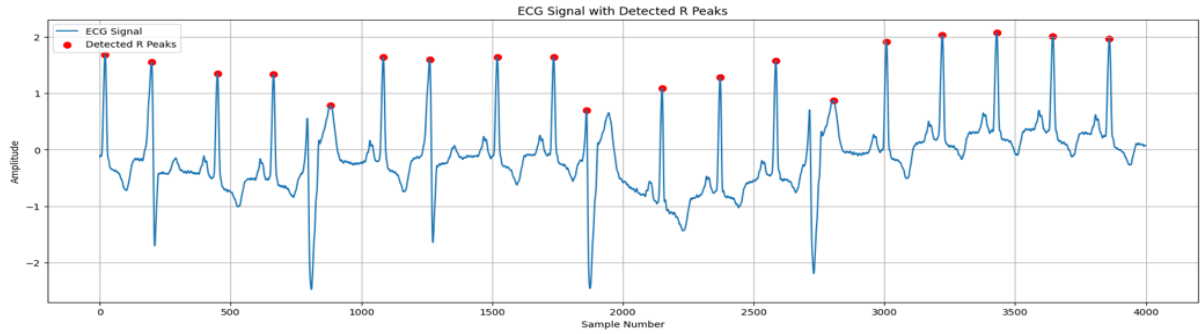

(c)

Figure 5. *Stages of our improved algorithm: (a) Original ECG, (b) Preprocessed signal after filtering, differentiation, squaring, and integration, (c) Detected R peaks.*

Table 1. *Comparison of Performance Metrics on Lead II*

Method	Sen (%)	Pre (%)	F1 (%)	FNR (%)	FPR (%)	Time (s)
Pan-Tompkins	96.56	98.44	97.45	0.13	0.25	51.96
RNN (No Preprocessing)	**98.73**	78.02	86.47	**0.02**	0.49	**42.32**
Improved Pan-Tompkins (RNN with preprocessing)	96.73	**99.88**	**98.24**	0.03	**0.03**	48.60

Table 2. *Comparison of Performance Metrics on Lead V5*

Method	Sen (%)	Pre (%)	F1 (%)	FNR(%)	FPR (%)	Time(s)
Pan-Tompkins	89.68	95.03	91.50	0.10	0.28	48.84
RNN (No Preprocessing)	**99.31**	68.17	80.12	**0.02**	0.53	**42.05**
Improved Pan-Tompkins (RNN with preprocessing)	93.60	**96.86**	**94.57**	0.04	**0.04**	48.08

Table 3. *Standard deviation of the baseline wander in original and filtered signals*

Signal	Original Signal	After Filtering (Pan-Tompkins)	After Filtering (Improved Pan-Tompkins)
1	0.1204	0.2051	**0.0681**
2	0.1387	0.2013	**0.0890**
3	0.8654	0.7386	**0.7123**
4	0.2038	0.1465	**0.1415**
5	0.2973	0.1916	**0.1895**
6	0.1779	0.1452	**0.1437**
7	0.1394	0.2111	**0.0684**
8	0.4581	0.3355	**0.3317**
9	0.5904	0.3888	**0.3156**
10	0.1500	**0.1254**	0.1278

A paired t-test was conducted to compare the standard deviation values obtained using the Pan-Tompkins bandpass filter and the improved Pan-Tompkins bandpass filter across the ten signal segments. The test revealed a statistically significant reduction in baseline drift using the improved method (p = 0.0273).

Figures 6, **7,** and **8** below show a visual comparison of ECG signals using the three experimental configurations. In these figures, false detections are indicated in green, and missed detections are shown in purple.

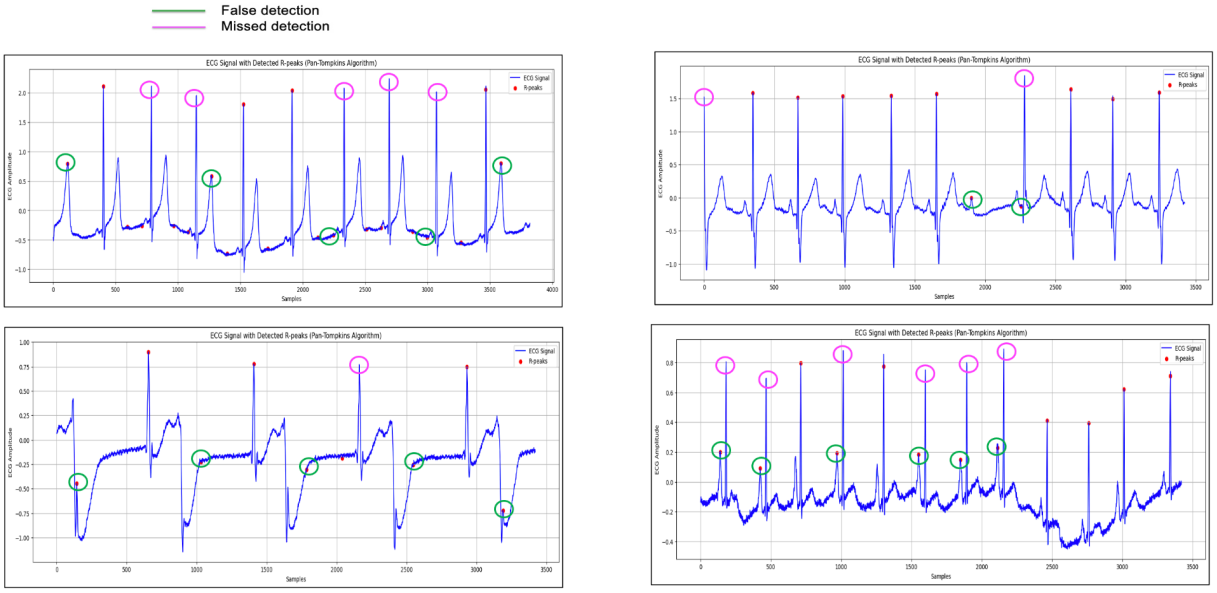

Figure 6. *ECG signals processed using the Pan-Tompkins algorithm.*

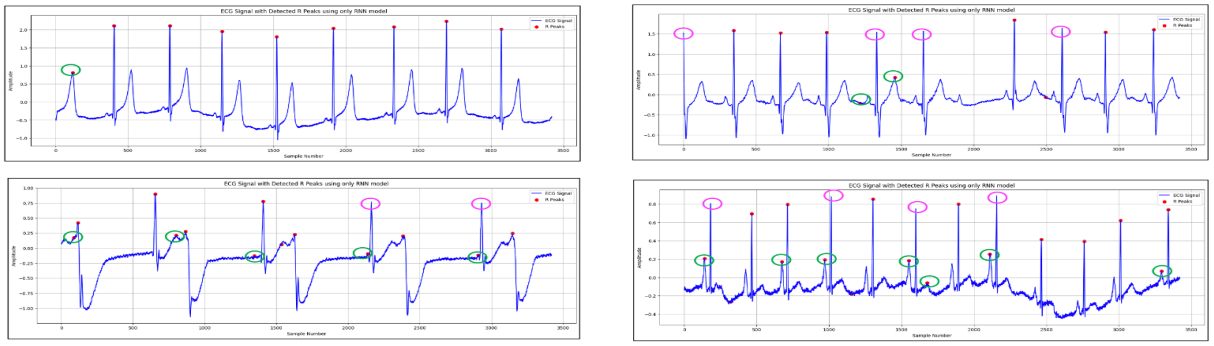

Figure 7. *ECG signals processed using the RNN with the unprocessed ECG signal.*

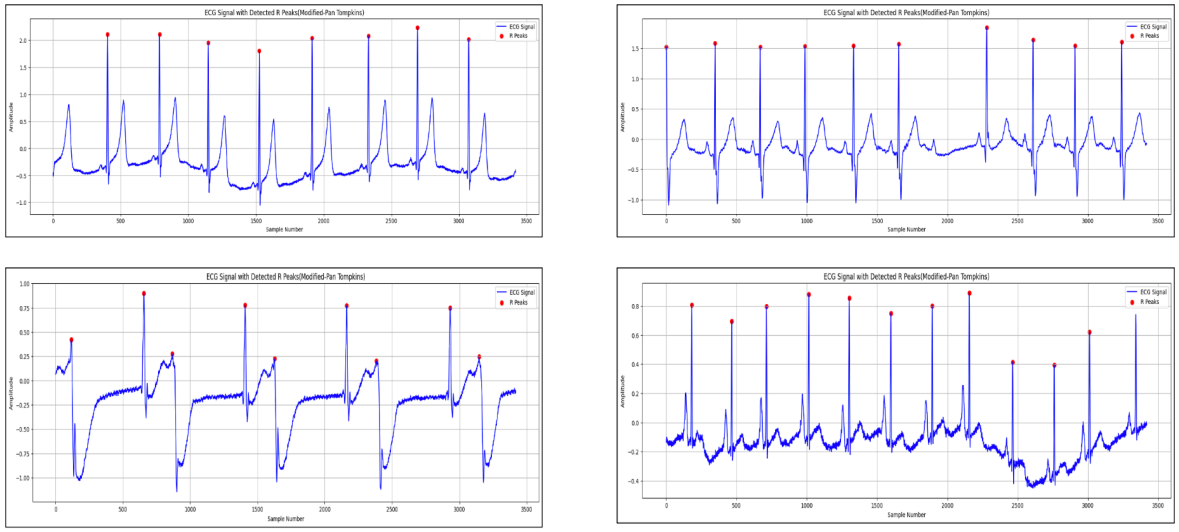

Figure 8. *ECG signals processed using our improved Pan-Tompkins algorithm.*

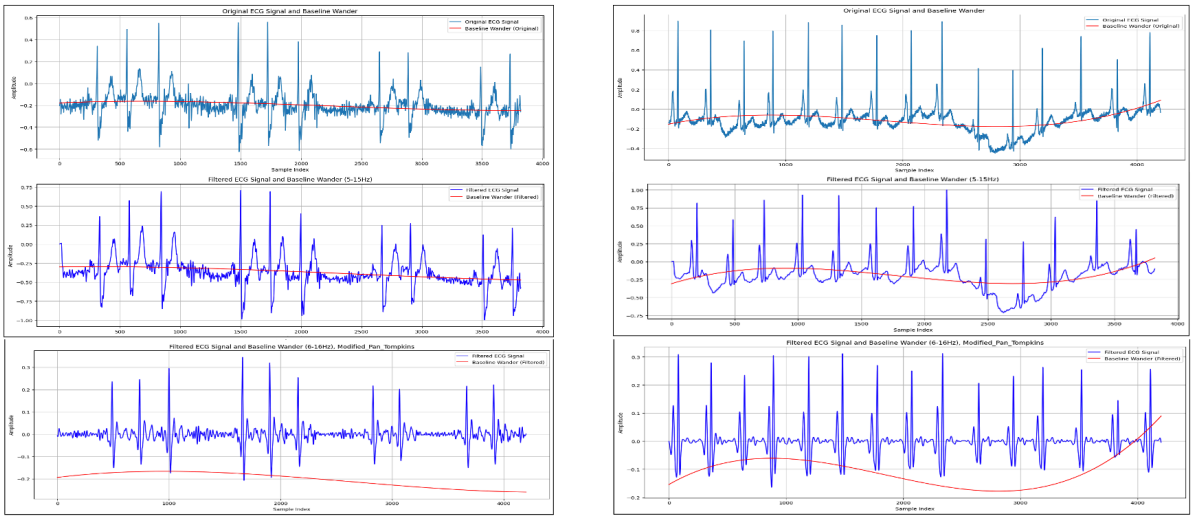

Figure 9. *Comparison of baseline wander reduction on first two ECG signals (Signal 1 and Signal 2). Each set shows the original signal, filtered signal using the standard Pan-Tompkins method, and filtered signal using the improved 6–16 Hz bandpass filter.*

5. Discussion

Figure 6, 7, and 8 illustrate the performance of the three experimental R peak detection methods: the Pan-Tompkins algorithm, an RNN model using the unprocessed ECG signal, and the improved Pan-Tompkins algorithm. The primary objective of this study was to address key limitations in the Pan-Tompkins algorithm, particularly with sensitivity to noise, signal variability, and real-time delay, while ensuring adaptability across diverse ECG morphologies.

Although reliable, the Pan-Tompkins algorithm (Figure 6) exhibited increased latency and was more susceptible to baseline wander and morphological variations, which impacted detection accuracy under non-ideal conditions. Its reliance on fixed thresholds made it less effective when processing ECG signals with varying amplitudes or irregular morphologies.

The RNN model, using the unprocessed ECG data (Figure 7), demonstrated strong sensitivity and specificity, learning generalized features directly from the signal. However, the lack of preprocessing made it vulnerable to noise, resulting in inconsistent heart rate estimations and lower precision. This inconsistency became more evident in signals with irregular morphologies, where the model failed to generalize effectively, leading to false detections and missed peaks.

The proposed improved algorithm (Figure 8) significantly enhances signal quality before feeding it into the RNN. This led to a reduction in the standard deviation of baseline drift (Figure 9), yielding a cleaner ECG waveform without compromising the morphological features essential for accurate R peak detection. To quantify this improvement, a paired t-test was conducted on the baseline standard deviation values from ten ECG segments filtered using both the Pan-Tompkins and the improved bandpass methods. The results showed a statistically significant reduction in baseline variability with the improved filter, confirming the method's robustness against low-frequency drift. With reduced noise interference and improved signal clarity, the RNN was better equipped to detect peaks consistently across different ECG morphologies.

Furthermore, this preprocessing pipeline contributed to a notable reduction in execution time, which directly translated to lower latency. To further strengthen detection accuracy, a search-back mechanism was incorporated to allow the system to recover missed peaks. The search-back logic dynamically adjusts based on signal variations, boosting recall by capturing peaks that may have been skipped due to transient noise, amplitude fluctuations, or atypical morphology. Importantly, this was achieved without significantly increasing processing time, ensuring that the algorithm remains computationally efficient and suitable for real-time use. The combined improvements introduced in this study demonstrate the potential for a more robust, adaptive, and efficient R peak detection method, effectively addressing key limitations of conventional algorithms and enhancing performance under diverse physiological conditions.

This study, however, has some limitations. The algorithm was evaluated only on a single database (MIT-BIH Arrhythmia Database), which may limit generalizability. Cross-validation was not performed, affecting the assessment of robustness. The method has also not yet been deployed in real-world clinical or community settings, which is important to evaluate practical feasibility and impact. Future work should focus on implementing the algorithm in community health settings across LMICs, where accessible and reliable ECG screening can play a vital role in early diagnosis and intervention. To enhance robustness and generalizability, subsequent studies should incorporate k-fold cross-validation and evaluate performance on larger, more diverse ECG datasets, including locally sourced datasets from LMIC populations. Performance reporting should include variability measures, such as the standard deviation of precision, recall, and F1-scores, to provide a comprehensive assessment of reliability.

By prioritizing low computational complexity and robustness to noisy acquisition environments, this approach directly addresses the constraints of ECG deployment in primary healthcare facilities across LMICs.

6. Conclusion

This study demonstrates that integrating the Pan-Tompkins algorithm with a slight modification to the bandpass filter and an RNN model enhances R peak detection accuracy while reducing baseline wander and processing latency. The modifications introduced led to improved signal quality, making the approach more robust against noise and morphological variations. These advancements support real-time applications such as wearable ECG monitoring systems, where reliability and efficiency are critical.

7. Recommendations

Future work should aim to validate and implement the algorithm in real-world settings, particularly in LMICs, and to assess its performance across larger, more diverse ECG datasets to ensure robustness and reliability.

Authors' Contributions

The project was conceptualized by EA and SDH. EA served as the principal author, conducted the experiments, and drafted the initial manuscript. SDH contributed to data processing and analysis. IA provided input and guided manuscript revisions. PEA provided supervisory oversight, refined the research objectives, and also guided manuscript revisions. All authors reviewed and approved the final manuscript.

Declaration of Interests

The authors declare that they have no known competing financial interests or personal relationships that could have appeared to influence the work reported in this paper.

References

1. Meng Qi et al. “Arrhythmia classification detection based on multiple electrocardiograms databases”. In: Plos one 18.9 (2023), e0290995.
2. Elsah Tegene Asefa, Tadesse Dukessa Gemmechu, Kedir Negesso Tukeni, et al. “Increase in Cardiovascular Disease Mortality in Low-and Middle- Income Countries: A Time for Action”. In: Ethiopian Journal of Health Sciences 35.1 (2025).
3. Oluwabunmi Ogungbe et al. “Medication adherence interventions for cardiovascular disease in low-and middle-income countries: a systematic review”. In: Patient preference and adherence (2021), pp. 885–897.
4. Homeyra Amiri et al. “Prediction of high-risk cardiac arrhythmia based on optimized deep active learning”. In: IEEE Access (2025).
5. K Kumar et al. “Electro Cardio Gram Using Different Machine Learning Techniques for Early Heart Attack Prediction”. In: Journal of Neonatal Surgery 14.19s (2025), pp. 769–776.
6. MAZ Fariha et al. “Analysis of Pan-Tompkins algorithm performance with noisy ECG signals”. In: Journal of Physics: Conference Series. Vol. 1532. IOP Publishing. 2020, p. 012022.
7. Feifei Liu et al. “The accuracy on the common Pan-Tompkins based QRS detection methods through low-quality electrocardiogram database”. In: Journal of Medical Imaging and Health Informatics 7.5 (2017), pp. 1039– 1043.
8. Luca Neri et al. “Algorithm for mobile platform-based real-time QRS detection”. In: Sensors 23.3 (2023), p. 1625.
9. Md Niaz Imtiaz and Naimul Khan. “Pan-Tompkins++: A robust approach to detect R-peaks in ECG signals”. In: 2022 IEEE International Conference on Bioinformatics and Biomedicine (BIBM). IEEE. 2022, pp. 2905–2912.
10. Jose Fernandez, Matthew Harris, and Carsten Meyer. “Combining algorithms in automatic detection of R-peaks in ECG signals”. In: 18th IEEE Symposium on Computer-Based Medical Systems (CBMS’05). IEEE. 2005, pp. 297–302.
11. Wenjie Cai and Danqin Hu. “QRS complex detection using novel deep learning neural networks”. In: IEEe Access 8 (2020), pp. 97082–97089.
12. Jiapu Pan and Willis J. Tompkins. “A Real-Time QRS Detection Algorithm”. In: IEEE Transactions on Biomedical Engineering BME-32.3 (1985), pp. 230–236. DOI: 10.1109/TBME.1985.325532.
13. Patrick S Hamilton and Willis J Tompkins. “Quantitative investigation of QRS detection rules using the MIT/BIH arrhythmia database”. In: IEEE transactions on biomedical engineering 12 (1986), pp. 1157–1165.
14. Yaqoob Ansari et al. “Deep learning for ECG Arrhythmia detection and classification: an overview of progress for period 2017–2023”. In: Frontiers in Physiology 14 (2023), p. 1246.
15. Estrella Everss-Villalba et al. “Noise maps for quantitative and clinical severity towards long-term ECG monitoring”. In: Sensors 17.11 (2017), p. 2448.